UNIVERSITY OF CALIFORNIA, SAN DIEGO

Compaction of Hydrogels by Compression or Permeation

A Thesis submitted in partial satisfaction of the requirements for the degree
Master of Science

in

Bioengineering

by

Sungil Hwang

Committee in charge:

Professor Robert L. Sah, Chair
Professor Shengqiang Cai
Professor Karen L. Christman

2016

The Thesis of Sungil Hwang is approved and it is acceptable in quality and form for publication on microfilm and electronically:

_____

_____

_____

Chair

University of California, San Diego

2016

Table of Contents

List of Abbreviations

AC: articular cartilage

ACI: autologous chondrocyte implantation

bCC: bovine calf chondrocyte

Calcein AM: calcein acetoxymethyl

CDC: Centers for Disease Control and Prevention

CTE: cartilage tissue engineering

DMEM: Dulbecco's modified Eagle's medium

dw: dry weight

ECM: extracellular matrix

FLS: fluid leaving surface

hMSC: human mesenchymal stem cell

MACI: matrix assisted autologous chondrocyte implantation

MF: microfracture

MSC: mesenchymal stem cell

OA: osteoarthritis

OAT: osteochondral autograft transfer

OCA: osteochondral allograft transplantation

P/S/F: Antibiotic-Antimycotic

PG: proteoglycan

sGAG: sulfated glycosaminoglycan

TGF-β: transforming growth factor – β

ww: wet weight

List of Figures

List of Tables

Acknowledgements

Primarily, I would like to acknowledge Dr. Robert L. Sah for his enthusiastic passion, guidance and support throughout this project. In addition, Eric Mendonsa, Erin Slattery and Evan Teng are greatly appreciated for their dedicated contributions and efforts. I am grateful to Felix Hsu, Aimee Raleigh, and Dr. Albert Chen for their wealth of advice and experimental knowledge which has helped me immensely in learning new techniques and acquiring excellent results. I also thank Van Wong for teaching me how to use Dynastat machine, fluorescence microscope, and other equipment in CTE lab.

Lastly, I cannot express how grateful I am to have such a caring and supportive family. I really thank my family, my dad, Dr. Jang-Yong Hwang, my mom, Young-Eun Shin, and my sister, Dr. Hyae-Jin Hwang, for their support, advice, and love; without them, I could not be where I am now.

ABSTRACT OF THE THESIS

Compaction of Hydrogels by Compression or Permeation

by

Sungil Hwang

Master of Science in Bioengineering

University of California, San Diego, 2016

Professor Robert L. Sah, Chair

Due to the limited ability for self-repair of articular cartilage (AC), many young and old patients experience discomfort and pain, significantly affecting their quality of life. Emerging treatments with tissue engineered cartilage are limited in large part by the inability to rapidly create and test new biomimetic tissue designs, with composition and function approaching normal tissue. Classical tissue engineering methods require substantial time for formation due to the time for cells to produce sufficient quantities of matrix A newly designed

bioreactor was tested for its ability to markedly increase the density of hydrogel solutions exuding fluid either by direct compaction with an applied constant pressure or permeation compaction with an applied constant fluid flow. Both methods resulted in a hydrogel that appeared much smaller and more opaque, with a final shape determined by that of the bioreactor walls or inserted spacers. The appearance was consistent with increased density based on compositional analysis, and retention of a large portion of the matrix component of the hydrogel. In addition, compressive and tensile load-bearing were improved in association with increased density. Relatively slow compaction by permeation resulted in mostly viable chondrocytes or mesenchymal stem cells, whereas relatively fast compaction by compression resulted in low cell viability. These studies demonstrate the potential for a new technology to rapidly create dense hydrogel materials of targeted geometry and density.

CHAPTER 1: ARTICULAR CARTILAGE

I. Structure and Function

Articular cartilage (AC) refers to the white and smooth connective tissue formed at the ends of bones that is avascular, aneural, and alymphatic, allowing it to withstand and endure harsh biomechanical environments. AC is largely comprised of three components: water, collagen, and proteoglycans. Water takes up about 65 – 80% of wet weight (ww) of the cartilage, and plays an important role in interacting with the solid components to determine the material properties of AC [4]. In addition, it has been noted that in osteoarthritic AC, an increase in water content in addition to decrease in concentration of other components, such as collagen and proteoglycans, results in diminished tensile stiffness [28, 47].

Collagen forms 10 – 20% of the ww of AC and consists of collagen II, III, VI, IX, X, XI, XII, and XIV, all of which contribute to the formation of an extracellular matrix (ECM). Specifically, collagen type II is the main collagen component and provides the tensile strength for mammalian cartilage. In addition, three types of collagen, type II, IX, and XI, become cross-linked to form a heteropolymer and the quantitative change in their compositions was detected with maturation from fine fibrils of young cartilage to thicker and differentiated mature cartilage [25, 26]. Thus, the material properties of AC can be altered by the composition of collagen types.

Lastly, proteoglycan composes 10 – 20% of the ww of AC and contributes to compressive stiffness [11]. The major proteoglycan in cartilage called aggrecan consists of glycosaminoglycans attached to a core protein. The proteoglycans in AC are negatively charged at physiological pH due to sulfonate and carboxylate groups, resulting in attraction of positively charged counter-ions within the AC matrix [15]. This property keeps cartilage neutral in physiological conditions and increases its osmolarity [51]. Overall, the three components of AC are important factors for defining its characteristics and are key to a successful tissue engineering solution to OA.

Highly specialized cells called chondrocytes reside and are dispersed within ECM. Originating from mesenchymal stem cells (MSC), chondrocytes compose about 2% of the total volume of AC and produce and maintain the extracellular matrix of cartilage [2, 53]. On the other hand, the fact that chondrocytes have a limited propensity to replicate and are difficult to culture without losing their phenotype adds a complication to their use in cell-based tissue engineering applications. Chondrocytes display different shapes and density within the various zones of AC defined as the superficial, middle, deep, and calcified (See Figure 1.1). The superficial, or tangential zone refers to the first 10 - 20% layer of the total articular cartilage from the articular surface. This zone contains densely packed collagen fibers aligned with the surface in addition to high number of the flattened chondrocytes. This dense layer of collagen fibrils, oriented tangentially, and cells helps to distribute shear, tensile

and compressive forces imposed by articulation, protecting the sub-surface tissue layers. The middle zone, just below the superficial zone, comprises 10 – 40% of the total articular cartilage thickness and contains collagen fibrils that are thicker and oriented obliquely, and spherical chondrocytes at low density. This zone serves as a structural connection between the superficial and deep zone. The deep zone, representing the remaining 80% of the total articular cartilage volume, is characterized by the lowest water content, the highest proteoglycan content, and thick collagen fibrils oriented in radial direction. The chondrocytes are also arranged in columns, in the same direction as the collagen fibrils. The high density of proteoglycan allows the cartilage to bear large compressive stress. The calcified zone, separated from the deep zone by the tide mark, connects the collagen fibers in the deep zone to the subchondral bone securing the cartilage to bone. The chondrocytes in the calcified zone are relatively few and hypertrophic in phenotype [67].

II. Problems

There are two well-known mechanisms for natural cartilage repair. Intrinsic healing depends on the proliferation of chondrocytes and production of proteoglycans and collagen. Extrinsic healing requires cartilaginous metaplasia of new connective tissue formed by mesenchymal elements from subchondral bone. Other possible mechanism suggests that a wave-like flow of matrix is generated to extend into the region of defect [24]. Despite these mechanisms,

adult articular cartilage has a very limited capacity for self-repair when damaged [46]. Once damaged, it is difficult to naturally regenerate new cartilaginous tissue for replacement, in part due to the avascular nature of the AC tissue. The inability of AC to self-repair imposes great trouble and inconvenience on our daily life. As a result, many young and old patients suffer from focal cartilage damage and osteoarthritis, causing inconvenience, discomfort, and pain [5, 32, 73]. The quality of life of these patients was significantly affected while a proper treatment is still a challenge [31, 65].

III. The Current Approach

There are several surgical procedures to treat focal cartilage defects. Chondroplasty treatments remove a small region of damaged cartilage, thus allowing new cartilage to grow at the site. The mircofracture (MF) technique not only removes the damaged tissue but also creates holes in the subchondral bone to stimulate cartilage growth around the tissue from mesenchymal cells. MF is known to be minimally invasive and cost effective surgical procedure with a relatively short recovery time. The majority of MF treated patients, however, predominantly had fibrocartilage growth within the operated region while only 10% had hyaline cartilage [40]. Other techniques include osteochondral autograft transfer (OAT) and osteochondral allograft transplantation (OCA). OCA facilitates transplantation of a donor's cartilage attached on the subchondral bone to a damaged region of a patient while OAT transfers healthy

cartilage of the patient from a less load bearing part of the body to the damaged area. One of the advantages of these techniques is that mature hyaline cartilage is immediately accessible in the defected region after surgery [60]. However, OCA and OAT treatments are limited by the amount of donor cartilage tissue available for the repair. Lastly, autologous chondrocyte implantation (ACI) is another surgical procedure used to treat damaged cartilage and involves three steps: harvesting cartilage tissue to isolate chondrocytes from the patient, followed by *in vitro* cell culture for several weeks, and, lastly, seeding of the cultured chondrocytes onto the damaged area for new cartilage formation.

Younger patients with single defects larger than 2 cm^2 had the most effective result from ACI [9, 13, 56]. However, since ACI is an expansive treatment associated with longer recovery time and the possibility for a secondary operation due to graft hypertrophy of the first generation ACI treatment, in addition to requiring two open arthrotomies [60]. Figure 1.2 demonstrates three available methods for ACI. Overall, none of these methods has been proven to effectively produce natural hyaline cartilage in clinical application.

One of the challenges in cell based tissue engineering treatments is the expansion of chondrocytes through *in vitro* culture to a sufficient number. The seeding density necessary within a scaffold to produce cartilage has been reported to be 10-13 x 10^6 cells/cm^3 and the optimal density for the best mechanical properties of yielded tissue is at 60 x 10^6 [18, 21, 49, 50, 70, 71].

To yield such a high number of cells, cell culture expansion is essential and must be conducted properly for clinical use. Otherwise, standard cell culture in monolayer seems to induce dedifferentiation of chondrocytes and transformation into more fibroblast-like cells producing more collagen type I instead of collagen type II [44]. As an alternative cell source, MSCs are known to differentiate into various cell types including chondrocytes, osteoblasts, myocytes, and adipocytes. Due to their multipotency and accessibility, MSCs show great potential for cartilage tissue engineering [19]. There have been many efforts to reform tissues using MSCs for implantation by inducing differentiation with media containing transforming growth factor-β (TGF- β) [57]. Overall, there are three methods that can facilitate the use of MSCs. First, MSCs are loaded into a scaffold and, after short period of incubation and cell attachment, the scaffold is transplanted. Second, the cell-scaffold is cultured with inducing media for a week or two, and then transplanted into the desired site. Third, the scaffold is implanted to allow the targeted cells to attach and allows to mature in vivo [19]. Kadiyala *et al* was able to show bone formation in the femora of adult rats 4 weeks after implantation of an MSC embedded scaffold [38]. Although there have been great improvements in the use of MSCs in clinical application, several challenging problems such as inflammatory response and source selection, still remain as unsolved [72].

In addition, a scaffold material can contribute greatly to initial functional mechanical properties, mass transport, and cell interaction in a tissue

engineered construct [33]. Chaipinyo *et al* showed that chondrocytes cultured in collagen type I scaffold after 4 weeks maintained their phenotype and synthesized a cartilage-like matrix [20]. Thus, three dimensional cultures within natural scaffolds including collagen, fibrin, agarose, alginate, chitosan and hyaluronan have been extensively studied to improve the phenotype and protein expression of cells as well as a carrier of cells [23]. Polymer type scaffolds, such as polyglycolic acid and polylactic acid, have also been studied as substrate for chondrocytes, resulting in high resistance to loading [45]. However, the toxicity of such monomers is an inherent limitation [66]. Conversely, chondrocytes can proliferate readily within hyaluronan based polymers without eliciting an inflammatory response, but the polymer degrades within 4 months [58]. Accumulation of various proteoglycans including aggrecan as well as type I and II collagen was observed within scaffolds made of hyaluronan and type I collagen in the presence of growth factors such as TGF-β [3]. Chitosan is another candidate for tissue engineering material to be used with chondrocytes since it can induce them to maintain their spherical shape and to synthesize aggrecan and type II collagen [42, 63]. As cells behave differently in various scaffolds, it is important to understand how the cell behavior changes in different three dimensional environment to properly engineer and develop cartilaginous constructs.

In an effort to create a biomimetic tissue-like constructs, conventional tissue engineering methods depend on cells to produce native matrix molecules

and deposite them within the carrier scaffold, often taking several weeks to complete [34]. The design of biomimetic collagen gel scaffolds with embedded cells had been studied but failed to achieve mechanical stability [27, 41]. These cell-dependent methods are not only time consuming, but also costly and the material properties of the scaffold are difficult to control. Replacing the carrier type scaffold, Brown *et al* showed a fabrication method of dense scaffold using collagen gel by plastic compression [14]. In plastic compression, the direct manipulation of matrix scaffold increases the density of a collagen construct by taking out most of interstitial fluid content. The advantages of this method include fast production of natural matrix scaffolds which have controlled matrix density and dimensions, and with that, corresponding mechanical and biological properties, with the possible integration of cells. Other studies using this method were compared in Table 1.1. Moreover, with a collagen density gradient, cell proliferation and cell migration were increased compared to that in hyperhydrated gel [22]. The compressive properties of engineered constructs can be improved by adding proteoglycan (PG) containing sulfated glycosaminoglycan (sGAG), and collagen-rich particles, with a 4:1 ratio of collagen to PG which mimics the compositional ratio of natural AC [30]. These results show the potential of engineering a biomimetic tissue-like construct using this approach.

IV. Figures

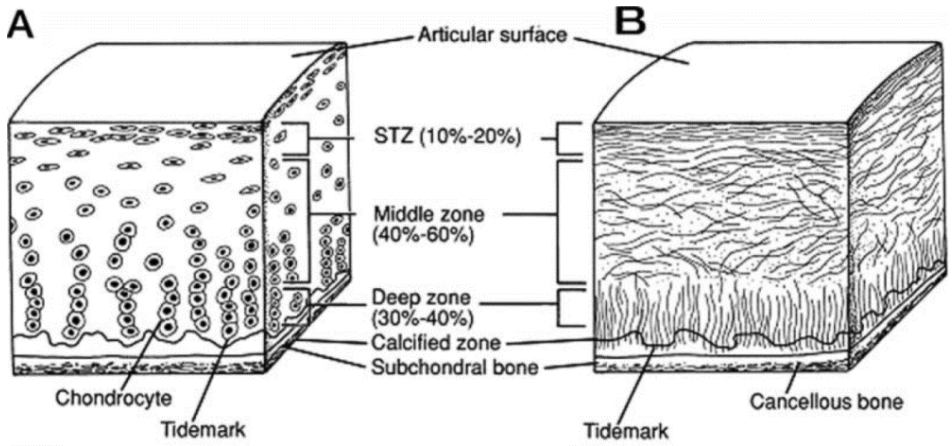

Figure 1.1. Schematic diagram of cross sectional view for a healthy articular cartilage. (A) Cellular organization in the zones of articular cartilage (B) Collagen and fiber architecture [16]

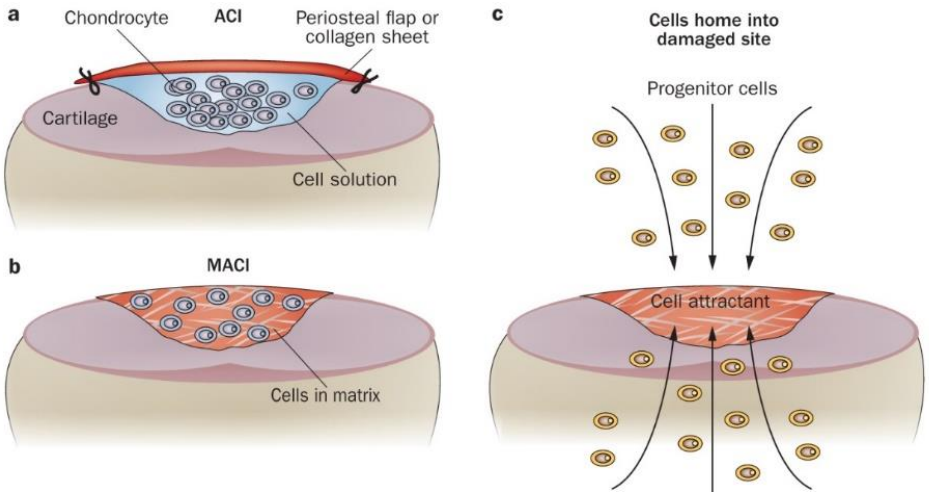

Figure 1.2. Schematic diagram of ACI process. (a) The expanded chondrocytes from a biopsy sample are implanted as suspension to a cartilage defect and covered with periosteal flap or collagen sheet to prevent from leaking. (b) For matrix assisted ACI (MACI), the chondrocytes are already placed in the matrix with structural stability at the time of implantation. (c) A new in situ engineering strategy to implant a cell-free matrix that contains local factor delivery systems for progenitor cell recruitment and differentiation is shown [61]

Table 1.1. Comparison of studies.

Study	Independent Var.									Dependent Var.		
	Method			Duration [min]	Shape	Pore size [um]	Material	C_i [mg / ml]	n	C_f [mg / ml]	h [mm]	Cell
	Compact type*	Load [g]	Flow rate [mm / min]									
Brown et al [14]	compression	10 - 50	n/d	~5	□	50	col type I	1.7	3 - 20	n/d	0.03	n/d
Han et al [30]		n/d	0.10	~27	○	2	col type II agarose PG	10	5	25	0.3	viable
Blum et al [12]		50 - 60	n/a	n/d	□	50	collagen oligomer atelocollagen telocollagen	3.5	7	3.5-24.5	0.35	viable
Sungil	compression	5000	-	~15	○	0.2	agarose col type I	2, 5	3	20-100	0.13-3.6	viable
	permeation	-	0.34	~38	○		col type I	2	1	40	n/d	

CHAPTER 2: `COMPACTION OF HYDROGELS BY COMPACTION OR PERMEATION

I. Introduction

Tissue engineered cartilage is needed for the repair of both focal defects and large areas of the articulating surfaces. Focal cartilage damage and osteoarthritis cause pain and dysfunction for patients, especially adults with aging [5, 32, 73]. Their quality of life has been significantly affected and the treatment still remains as a challenge [31, 65]. The biomechanical function of cartilage depends on a sufficient density of proteoglycan and collagen matrix components. The increase in collagen concentration during normal development results in improvements in both compressive and tensile load-carrying properties of cartilage [74, 75]. However, traditional methods of cartilage tissue engineering, involving deposition of matrix components by indwelling cells, require long time periods and often fail to achieve functional mechanical properties [27].

Recent studies introduced the concept of increasing matrix density by including substantial components of matrix and then controlled exudation of fluid. Brown et al suggested that a plastic compression of collagen type I gel resulted in rapid formation of a dense scaffold [14]. This study introduced a simple and fast method of fabrication while cell viability significantly decreased after desiccation. Another study looked at the compressive properties that were successfully improved by obtaining a high level of aggrecan in the constructs

and by compaction [29, 30]. This finding can be useful in improving the biomechanical properties of constructs. Creating both acellular and cellular constructs via densification also has been possible although preparation of collagen oligomers adds complexity in compaction process [12]. These findings provide a novel engineering approach to creating a tissue-like graft. The comparison of these studies in addition to this paper was summarized in Table 3.6.

Cartilage can be compacted by applying load in a number of ways with a variety of boundary conditions, including by direct compression of the tissue surface and by applying fluid flow. With cartilage modeled as a biphasic material, the creep and stress relaxation responses of articular cartilage to confined compression with a free-draining porous platen were analyzed, with the result being due primarily to “diffusional drag of relative motion of the interstitial fluid with respect to solid matrix” [52]. The flow of fluid within and through cartilage can be described by Darcy’s equation for porous media with permeability modulated by the degree of tissue compaction and fixed charged density [43, 48]. The application of fluid flow through cartilage, backed by a free-draining porous platen can affect mass transport within constructs, including the distribution of aggrecan [39]. These biomechanical models of compaction give insight into the nature of compaction by application of compression or fluid flow to a radially-confined construct, with fluid exudation through a porous restraining surface.

A variety of hydrogels have been used both as model systems to study cartilaginous tissue formation and cell interactions with tissue. Agarose, a polysaccharide polymer material extracted from seaweed, has long been used for three-dimensional cultures of cells and tissue models. It (1) has minimal intrinsic interaction with mammalian cells [62], (2) helps maintain the phenotype of chondrocytes *in vitro* [10], and (3) promotes formation of cartilaginous tissue [17]. Collagen is the most common natural polymer in our body and comprises up to ~20% of the wet weight in articular cartilage. In addition to its mechanical properties, collagen has a number of biological properties, modulating cell adhesion and allowing natural degradation by endogenous enzymes [55]. While the predominant type of collagen in cartilage is type II, a substantial amount of type I collagen is present in cartilage repair as component of fibrocartilage [54]. For cartilage tissue engineering, chondrocytes and MSCs are often analyzed. Chondrocyte, naturally found in articular cartilage, produces abundant ECM, and can be isolated and culture-expanded, and is the basis for the treatment of cartilage defects by autologous chondrocyte implantation [59]. The multipotency and accessibility of human MSC can also be beneficial in cartilage tissue engineering since differentiation can be induced within hydrogels [8]. Thus, hydrogels based on collagen and agarose, and incorporated cells including chondrocytes and MSCs, serve as a useful and important model system for cartilage tissue engineering.

II. Hypothesis and Aims

The overall hypothesis is that a bioreactor can be used in either a direct compression or permeation mode for creating compacted hydrogel constructs with controlled indices of structure, composition, function, and metabolism. The aims for these studies were to determine effects of (1) direct compaction of agarose and collagen hydrogels on structure, composition, mechanical properties, and cell viability, (2) direct compaction of agarose and collagen hydrogels with spacer on structure, composition, and mechanical properties, and (3) permeation compaction of collagen hydrogels on composition and cell viability.

MATERIALS AND METHODS

I. Experimental Design

Study 1: The effect of collagen density on biomechanical properties of a compacted construct

A. Preparation of Compacted Constructs with Various Concentrations

To examine the effect of density on biomechanical properties of compacted constructs, agarose and collagen were used with different target concentrations (C_f) (Table 2.1). In Exp I, agarose gels with two different concentrations were compacted and, in Exp II, collagen gels with three different concentrations.

B. Preparation of Cellularized Construct

Additional experiment (Exp III) was completed to determine the effect of direct compaction on cell viability using bCCs and hMSCs. The bioreactor was assembled with sterility. hMSCs were obtained (Lonza, Switzerland), cultured on monolayer with 1X DMEM containing high glucose (4 g/L) concentration, 10% FBS, and 1X P/S/F, and maintained in a water jacketed incubator at 37°C and 5% CO_2. The isolated bCCs harvested from bovine calf knee cartilage were used at passage 2 and cultured at high density (250,000 cells/cm^2) with complete media (1X DMEM containing low glucose concentration, 10% FBS, 1X P/S/F, 10mM HEPES (UCSD Core Bio Service, CA), 0.1mM non-essential amino acids (Sigma-Aldrich, MO), 0.4mM L-proline (Sigma-Aldrich, MO), and

0.5mM ascorbate (Sigma-Aldrich, MO)). Instead of 1X DMEM during the preparation of collagen solution, the cell suspension solution containing either bCCs or hMSCs was mixed with the other reagents. The sample size (n=1) was sufficient as a pilot study to see the effect on cell viability. A final cell density of 100,000 cells/ml after mixing and a target collagen concentration of 20mg/ml was seeded into the bioreactor. After two hrs of incubation at 37°C and 5% CO_2, the collagen gel with cells was compacted using the piston, applying 180 kPa of load until the complete compaction.

Study 2: Engineering a compacted construct – controlled thickness and diameter during agarose and collagen compaction

Spacer with a thickness (h), 3.18mm, of three inner diameters (ID), 6.4, 9.6, and 12.7 mm, was designed (Figure 2.2) to control dimensions of compacted constructs. Thus, the effect of spacers with various dimensions on a compacted construct was studied. Both agarose (Exp IV) and collagen gels (Exp V) were compacted with spacers (Table 2.2). Spacers were placed on the bottom before the solution was seeded and compacted in the bioreactor (Figure 2.1 (A)).

Study 3: Creating a cellularized collagen construct via permeation compaction

A. Bioreactor Assembly for Permeation Compaction

The effect of the permeation compaction method on cell viability in high dense collagen construct was studied (Exp VI). The compaction bioreactor was assembled under sterile conditions. A porous titanium frit was sonicated for at least 10 min, autoclaved, and layered with 0.2µm pore size Whatman Nuclepore Track-Etched Membrane (Sigma-Aldrich, MO) and then with 40µm pore size cell strainer (BD Falcon, CA) to form a filter. The double layered filter was placed on the bottom of the bioreactor at the fluid leaving surface (FLS) [22]. It was kept hydrated with 1X Dulbecco's modified Eagle's medium (DMEM; Gibco, Paisley, UK) containing low glucose (1g/L) concentration, 10% fetal bovine serum (FBS; Omega Scientific, CA), and 1X Antibiotic-Antimycotic (P/S/F; UCSD Core Bio Service, CA) to prevent the generation of air bubbles inside the frit. This was done by filling the bottom chamber with 3ml of media and putting a few drops of the media on the top of the filter. The peristaltic pump (Watson Marlow, England) was used with 0.062" ID X 0.125" OD silicon tubes (Nalge Company, NY) connected to the bottom outlets of the bioreactor instead of the piston. A reservoir was connected to the end of the tubes to collect the liquid filtrate. See Figure 2.3 for a schematic diagram of the bioreactor setting for the permeation method.

B. Cell Preparation

The hMSC at passage 5 was obtained (Lonza Group, Switzerland), cultured on monolayer with 1X DMEM containing high glucose (4g/L)

concentration, 10% FBS, and 1X P/S/F, and maintained in the water jacketed incubator at 37°C and 5% CO_2. The bCCs were isolated from the harvested bovine calf knee cartilage obtained from a local vendor. To briefly describe the cell isolation procedure, about 1g of cartilage tissue was digested with pronase from *Streptomyces griseus* type XIV (Sigma-Aldrich, MO) followed by collagenase P digestion from *Clostridium histolyticum* with Lypholizate (Roche Applied Science, Germany). The average yield of bCCs was approximately 2.5 million cells per gram of cartilage tissue. The isolated bCCs were seeded at high density (200,000 – 250,000 cells/cm^2) on monolayer, cultured with the complete media (1X DMEM containing low glucose concentration, 10% FBS, 1X P/S/F, 10mM HEPES (UCSD Core Bio Service, CA), 0.1mM non-essential amino acids (Sigma-Aldrich, MO), 0.4mM L-proline (Sigma-Aldrich, MO), and 0.5mM ascorbate (Sigma-Aldrich, MO)), and maintained in the water jacketed incubator at 37°C and 5% CO_2. The bCCs were used for compaction within a week after the isolation to avoid a dedifferentiation.

C. Cellular Collagen Construct Formation

The collagen solution of 2mg/ml was prepared with the final cell density of 500,000 cells/ml. Seeding volume of 2.66 ml was determined by the target concentration of 40 mg/ml in assumed final dimension of the construct as 18.7mm diameter and 1.0mm thickness. Therefore, 20 fold increase of density was targeted. The cellular collagen solution was seeded into the bioreactor and

incubated at 37°C/5%CO_2 for at least 60 min for gelation and attachment of cells to collagen fibril. The bioreactor was connected to the peristaltic pump to draw fluid out at a rate of 43 µl/min from the bottom (Figure 2.3 (B) and (C)).

II. Methods

A. Bioreactor Assembly for Direct Compaction

The compaction bioreactor was assembled in sterile condition. A porous titanium frit was sonicated for at least 10 minutes, autoclaved, and layered with a 0.2µm pore size Whatman Nuclepore Track-Etched Membrane (Sigma-Aldrich, MO) and then with a 40µm pore size cell strainer (BD Falcon, CA) to form a filter. The double layered filter was placed on the bottom of the bioreactor. It was kept hydrated with 1X PBS for the agarose gel compaction and with 1X Dulbecco's modified Eagle's medium (DMEM; Gibco, Paisley, UK) containing low glucose (1 g/L) concentration, 10% fetal bovine serum (FBS; Omega Scientific, CA), and 1X Antibiotic-Antimycotic (P/S/F; UCSD Core Bio Service, CA) for the collagen gel compaction to prevent generating air bubbles inside the frit. This was done by filling the bottom chamber with 3ml of media and putting a few drops of the media on the top of the filter. Another double layered filter was assembled and placed on the piston at the fluid leaving surface (FLS) [22]. The piston with filter was hydrated in media until use. Figure 2.1 presents a schematic diagram of the work flow using the bioreactor with piston.

B. Preparation of Compacted Agarose Construct

SeaPlaque agarose (FMC BioProducts, ME) was mixed in 1X PBS to make the desired agarose solution and heated while stirring until dissolved completely. The clear agarose solution was seeded into the bioreactor while hot and cooled down for 2 hours to be gelled at room temperature. The mechanical loading of 180 kPa with the piston was applied to the gel overnight until it was completely compacted. The compacted construct was taken out for further analysis.

C. Preparation of Compacted Collagen Construct

Rat tail collagen type I solution (4mg/ml) (Corning Inc., NY) was diluted to 3mg/ml with 0.02M acetic acid (UCSD Chem Stockroom, CA) and kept at 4°C. 6X DMEM solution was prepared by diluting from 10X DMEM (Sigma-Aldrich, MO). 1M NaOH (UCSD Chem Stockroom, CA) was added to 6X DMEM based on the predetermined concentration (11.11µl per 100mg total collagen used) to adjust the final pH to be 7.5. By mixing in ratio 2:10:3=pH'd 6X DMEM: 3mg/ml collagen solution: 1X DMEM, a final collagen solution of 2mg/ml was prepared. To vary the density of a final construct, different seeding volumes were determined based on the assumption that the final construct was compressed to 0.77mm thickness with 15.9mm diameter disc. As a result, the final volume of the construct was assumed to be 0.152ml. The collagen solution prepared at 4°C was seeded into the bioreactor and incubated for 2 hours at 37°C/5%CO_2

(Figure 2.1 (A)). After gelling, an additional 1X DMEM was filled to the final volume of 12.5ml. The collagen gel was compacted with the piston, applying 180 kPa of load until the complete compaction (Figure 2.1 (C)). The compacted construct (Figure 2.1 (D)) was removed for further analysis.

D. Biomechanical Testing

The compacted construct was placed in 1X PBS for one hour. The wet weight was measured and recorded. The specimens for tensile and confined compression testing were punched out from the construct as a dog-bone shape and circular disc, respectively. Dimension of the dog bone specimen was 12+mm X 1.8 mm X h mm (length X width of narrow region X height) while that of a circular disc was 6.4 mm or 9.6 mm diameter depending on the availability of the sample. The machine used for mechanical testing was a Dynastat mechanical spectrometer. During the equilibrium tensile testing, the dog bone specimen was extended from 0% to 20% strain for a ramp time of 400s followed by a relaxation for 3600s. Another extension of the sample occurred from 20% to 40% strain for a ramp time of 400s followed by a relaxation for 3600s. After acquiring data, the sample was stretched until break. During the oscillatory confined compression stress relaxation testing, the circular disc sample was placed in the confining chamber and compressed from 0% to 20% strain for a ramp time of 400s followed by a relaxation for 36000s and tested for oscillatory behavior at 0.01, 0.02, 0.05, 0.1, 0.2, and 0.5 Hz with 3, 2.6, 2.2, 1.8, 1.4, and

1 dynamic amplitude and 3 cycles. Another compression occurred from 20% to 40% strain and tested, followed by the relaxation from 40% to 0% strain for a ramp time of 60s followed by a relaxation of 3600s.

E. Dry Weight Measurement

The compacted constructs were measured for their physical dimensions as well as the ratio of dry to wet weight. Thickness was measured by AccuRange 200 Laser Displacement Sensor (Acuity, OR). At least five thicknesses at different points on the construct were measured to calculate an average thickness. The constructs were frozen and lyophilized overnight to measure the dry weight. For collagen construct, it was soaked in excess 1X PBS for an hour, frozen, and lyophilized overnight for the dry weight.

F. Cell Viability Assay

Cell viability within the compacted constructs was analyzed right after the completion of compaction. The compacted constructs as well as uncompacted construct controls were placed in complete media and assessed qualitatively for cell viability by live/dead staining (Life Technologies, CA). Fluorescence microscopy was used for viewing and images taken by Nikon D90 DSLR (Nikon, Japan).

III. Figures and Tables

A. Figures

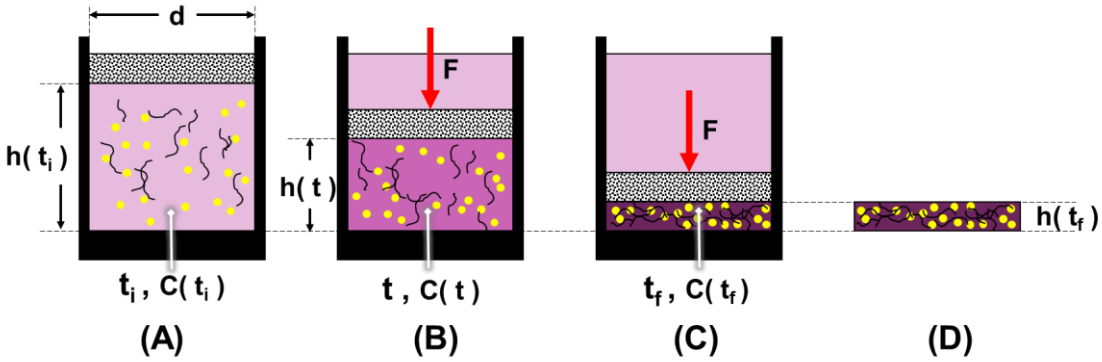

Figure 2.1. Overview of direct compaction method. (A) Hydrogel is seeded into the main chamber and includes medium (pink), matrix (black lines), and cells (yellow dots). (B) Piston with porous membrane is applied directly on the hydrogel with load, F. (C) Fluid is exuded from the gel, resulting in changes in concentration, C, of gel constituents and thickness, h, of gel. (D) Dense construct that is formed.

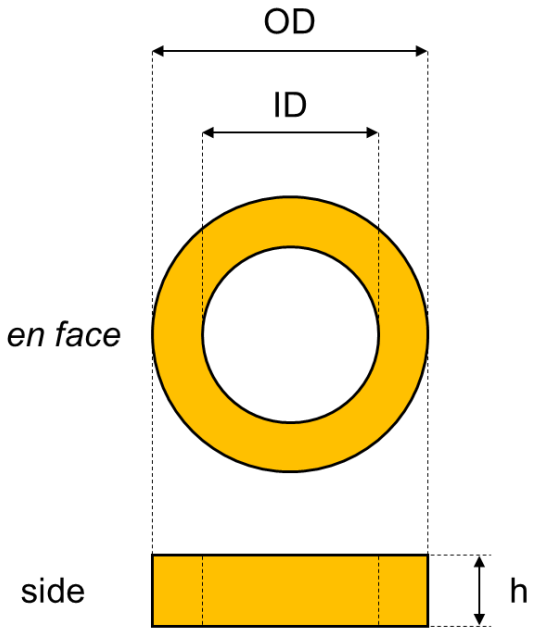

Figure 2.2. Geometry of spacer. OD: outer diameter, ID: inner diameter, h: thickness. OD is set as inner diameter of the main chamber, while ID is varied.

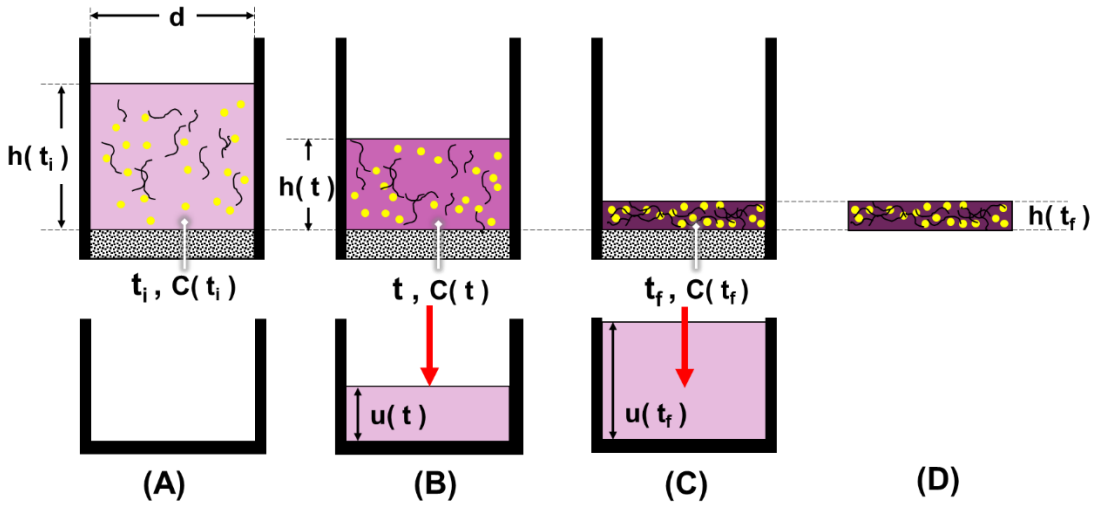

Figure 2.3. Permeation bioreactor schematic diagram. (A) Cellular collagen solution is seeded to the main chamber and incubated at 37°C. (B) The fluid content is taken out by a peristaltic pump via permeation. (C) The cellular construct is formulated and (D) is analyzed. (B), (C), and (D) are performed at 25°C.

B. Tables

Table 2.2. Experimental design for different target/final density of constructs. C_i: initial concentration, **C_f**: target concentration. Geometry of final construct was h=1.50 mm, d=12.7 mm.

Exp	Group	Material	C_i [mg / ml]	C_f [mg / ml]	Cell type	Compaction	Sample size (n)
I	01	agarose	2	164	-	direct	3
	02		5	411	-		3
II	01	collagen	2	20	-		3
	02		2	60	-		3
	03		2	100	-		3
III	01	collagen	2	2	-		1
	02		2	2	bCCs		1
	03		2	2	hMSCs		1
	04		2	20	bCCs		1
	05		2	20	hMSCs		1

Table 2.3. Experimental design (compaction with spacer). h: thickness of a spacer. ID: inner diameter of a spacer. C_i: initial concentration. C_f: target / final concentration. *Final volume was calculated based on the assumption that the construct forms within the spacer dimension.

Exp	Group	Material	h [mm]	ID [mm]	C_i [mg/ml]	C_f [mg/ml]	Comp-action	Sample size (n)
IV	01	agarose	-	-	5	5	-	1
	02		1.50	12.7	5	417	direct	1
	03		3.18	12.7	5	156		1
	04			9.6	5	272		1
	05			6.4	5	625		1
V	01	collagen	-	-	2	2	-	3
	02		1.50	12.7	2	20	direct	1
	03		3.18	12.7	2	8		1
	04			9.6	2	13		1
	05			6.4	2	30		1

Table 2.4. Experimental groups (permeation compaction). Geometry of final construct was h=1.50 mm, d=12.7 mm.

Exp	Group	C_i [mg / ml]	C_f [mg / ml]	Cell type	$C_{i,cell}$ [10^6 / ml]	Comp-action	Sample size (n)
VI	01	2	2	-	0	-	1
	02	2	2	hMSC	0.1	-	1
	03	2	2	bCC	0.5	-	1
	04	2	40	hMSC	0.1	permea tion	1
	05	2	40	bCC	0.5		1

RESULTS

I. Study 1: The effect of collagen density on biomechanical properties of a compacted construct

A. Formation of Compacted Agarose Constructs

The agarose constructs were successfully compacted in the bioreactor (Figure 3.1). The compacted constructs were opaque and structurally firm. Noticeable difference in appearance was not observed between groups. However, the edges were more transparent than the center (Figure 3.1 (B)). The thickness of the final constructs varied in each trial, resulting in high standard deviation (Table 3.1). In addition, the measurement of biomechanical properties through confined compression testing was inconsistent (Table 3.1). While the agarose compaction resulted in increase in final concentrations, leaking of agarose gels through top chamber was observed. As a consequence, inconsistent constructs were produced to cause very high difference in biomechanical properties (Table 3.1). As a preliminary experiment, the construct formation in the bioreactor by confined compression proved to be operable.

B. Formation of Compacted Collagen Constructs

The collagen constructs of various concentrations of collagen were successfully produced in the bioreactor using the direct compaction method (Figure 3.2). The translucent pink colored soft tissue-like constructs were

formed after compaction for all the experimental groups. All the constructs were circular discs with uneven thickness. Notably, the outer edge was thinner than the center. Qualitatively, II/03 was the most opaque construct, followed by II/02 while II/01 was transparent to some extent (Figure 3.2). Due to very soft and thin structure, II/01 was easily damaged and folded upon itself and was thus difficult to handle. Conversely, II/02 and II/03 were easy to handle due to their structural rigidity

C. Thicknesses and Concentrations

Paired t-test was performed to determine the significance of the effect of compaction. Thicknesses of II/01, II/02, and II/03 were reduced to 1.9% ($p<0.05$), 3.86% ($p<0.05$), and 2.65% ($p<0.05$) of their initial values, respectively. The significance of thickness difference across the samples was found from ANOVA test ($p<0.05$). Whereas, the collagen concentrations of II/01, II/02, and II/03 were increased by 28 ($p<0.01$), 32 ($p<0.01$), and 47 fold ($p<0.01$), respectively (Figure 3.11 (B)). The collagen concentrations of II/02 and II/03 reached their target concentrations, 60 ($p<0.01$) and 100 mg/ml ($p<0.01$), respectively, within one standard deviation while that of II/01 was overachieved ($p<0.01$) (Figure 3.11 (B)) No significance between groups for the concentration of collagen was found from ANOVA test ($p<0.07$).

D. Biomechanical Properties

The equilibrium tensile testing and oscillatory confined compression stress relaxation testing on Dynastat mechanical spectrometer were performed on the compacted constructs. The data listed on Table 2.3 shows the results of biomechanical tests. Two sample t-test (two tailed) was performed to determine significant differences between the two groups, II/02 and II/03. The significant difference was found for max load values (p<0.05) while differences between the groups of other parameters including H_{A0}, k_{p0}, peak stress, elongation at failure, failure strain, and stiffness at failure, were in significant (p>0.30). Statistical analysis on the biomechanical properties of the constructs measured from the oscillatory confined compression stress relaxation test and equilibrium tensile test suggests that a significance in max load exists between II/02 and II/03 (p<0.05). In addition, the mean of hydraulic permeability and failure strain were twice as high in II/03 than in II/02 (p>0.30), indicating the possible improvement in biomechanical properties.

E. Cellullarized Construct Formation and Cell Viability Test

Cellularized constructs, III/04 and III/05, were successfully produced. Both constructs were soft and flimsy, having similar characteristics to II/01. The live/dead assay was performed right after compaction. Approximately 7.3% cell viability was found for III/05 while no cells were alive for III/04 (Table 3.3). Some live cells for III/05 were observed under 10X magnification microscope (Figure 3.4 (A)).

II. Study 2: Engineering a compacted construct – controlled thickness and diameter during agarose and collagen compaction

A. Compacted Agarose Constructs with Spacers

The agarose gels were fully compacted with the spacers via uniaxial loading and the compacted constructs were successfully formed (Figure 3.6). The compacted constructs were shaped by the spacers and the hat part of the constructs (indicated in Figure 3.5) physically fit into the spacer. The diameter of the hat shaped part for all the constructs corresponded to the ID of the spacers used within one standard deviation. However, the heights (h) of the constructs were found to be higher than that of the spacers (Table 3.4). The constructs, especially the thinner parts, were easily broken during disassembly of the bioreactor, thus, forming uneven surfaces and edges.

B. Compacted Collagen Constructs with Spacers

The compacted collagen constructs were successfully produced using the spacers (Figure 3.4). The final constructs were pink circular disks. The center of the constructs was more opaque and intense color than the periphery. In addition, unlike the compacted agarose constructs, they were more round shaped. The thin peripheral aspects of the collagen constructs were soft, flimsy, and easily folded on thin peripheral part. They were very soft and easily folded. A denser core was formed and was opaque while the peripheral part was thinner and transparent (Figure 3.4 (C) and (D)), resembling a sunny side up egg. In

addition, the thickness of all the constructs was much less than the spacer thickness (Table 3.4). However, the diameter of the center for all the groups fit the corresponding ID of the spacers within one standard deviation.

C. Concentration and Thickness

The final concentration was determined from the ratio of dw to ww. The concentrations of the agarose constructs as well as that of the collagen constructs increased after compaction (Figure 3.12 (C) and (D)). Agarose contents that were not recovered in the constructs were found in the top chamber after compaction. The collagen concentrations increased by 7.1 – 21.4 folds. The significant decrease in thickness was observed for all samples (Table 3.2). Inner diameters of the constructs (ID) were decreased after compaction (Figure 3.12 (A) and (B)). Most of them were similar to their inner diameters of spacers within one standard deviation (Table 3.4) as well. Control group IV/02 had smaller ID than expected due to fragility of the construct (Figure 3.12 (A) ctrl).

III. Study 3: Creating a cellularized collagen construct via permeation compaction

A. Formation of Compacted Collagen Constructs

The high density collagen constructs were successfully produced in the bioreactor using permeation method (Figure 3.8). The shape of the compacted constructs was determined by the circular chamber of the bioreactor while that

of control groups were determined by 50 ml conical tubes in which they were seeded in for gelling. The color of all constructs was light pink. Difference in opacity was noticeable. Uniform opacity was observed for the controls while the opacity of other constructs, VI/04 and VI/05, were uneven as indicated by the intensity of color. In addition, bubbles inside all the gels were visible. The physical characteristics of the constructs were soft, fluidic, and gel-like after compaction. The duration of the complete compaction was about 37.5 min.

B. Live/Dead Assay

Cell viability in the constructs was analyzed by staining with the live/dead assay. Approximately >60% cell viability of the compacted constructs was counted (Table 3.5). The higher number of cells can be seen in Figure 3.9 (D) and (E) compared to (B) and (C), respectively. In addition, slight decrease in cell viability was measured between control groups and the experimental groups (Table 3.5). Neither live nor dead cell was detected on negative control group, as expected.

IV. Figures and tables

A. Figures

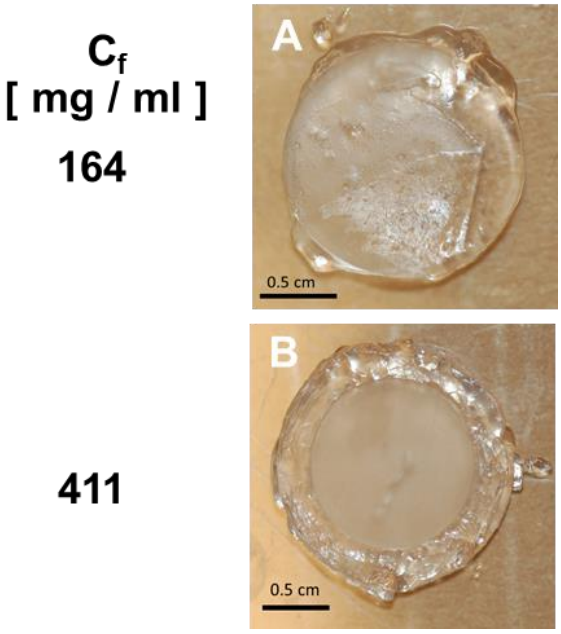

Figure 3.1. Compacted agarose constructs of direct compaction. Agarose gels were compacted to target **(A)** 164 and **(B)** 411 mg/ml after compaction.

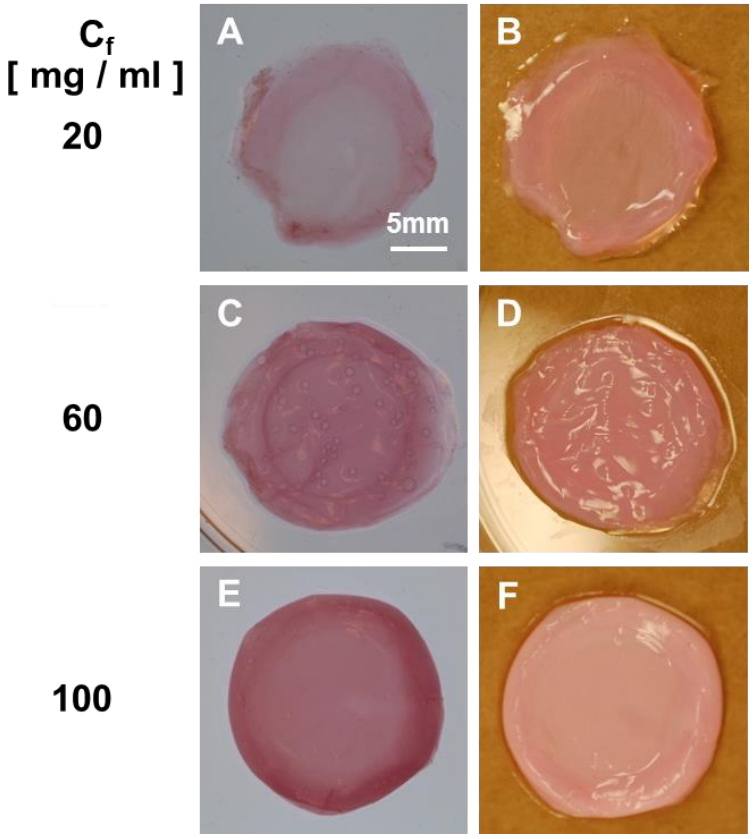

Figure 3.2. Compacted collagen constructs of direct compaction. Collagen compacted constructs with target concentration of **(A,B)** 20mg/ml, **(C,D)** 60mg/ml, and **(E,F)** 100mg/ml were formed. **(A,C,E)** Light background to show the opacity. **(B,D,F)** Solid background.

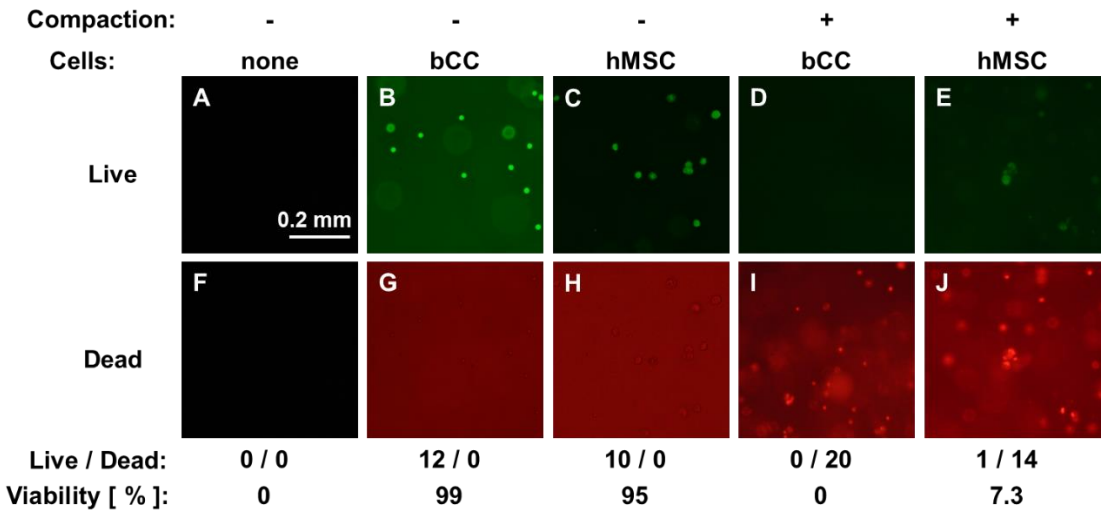

Figure 3.3. Effects of direct compaction on cell viability. (A-E) Green fluorescence indicating live cells. **(F-J)** Red fluorescence indicating the nuclei of dead cells.

.

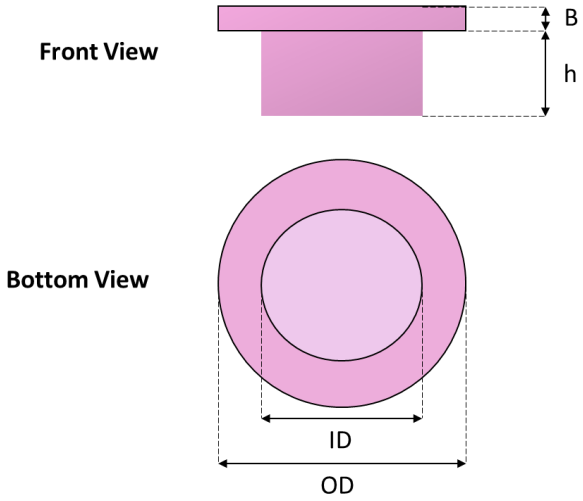

Figure 3.4. Schematic of construct geometry resulting from use of spacer. Layer of thickness, h1, and diameter, d1, were occasionally present above main construct of total thickness, h, and main diameter, d.

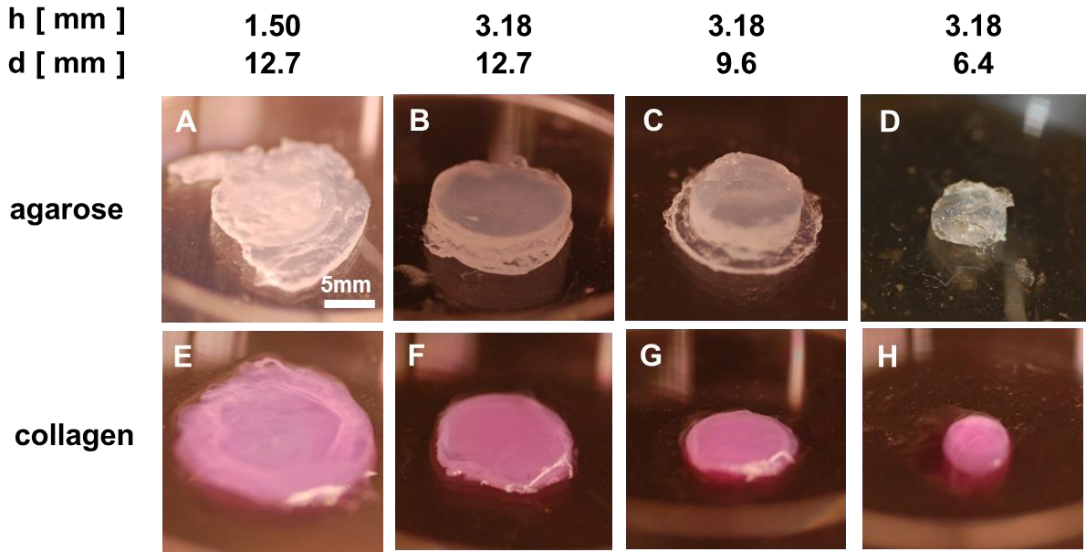

Figure 3.5. Effects of spacer on geometry of constructs formed by direct compaction. Constructs were formed with **(A-D)** agarose or **(E-H)** collagen, and with **(A,E)** standard spacer or **(B-D, F-H)** spacer with height, h=3.18mm, and diameter, d, **(B,F)** 12.7mm, **(C,G)** 9.6mm, or **(D,H)** 6.4mm.

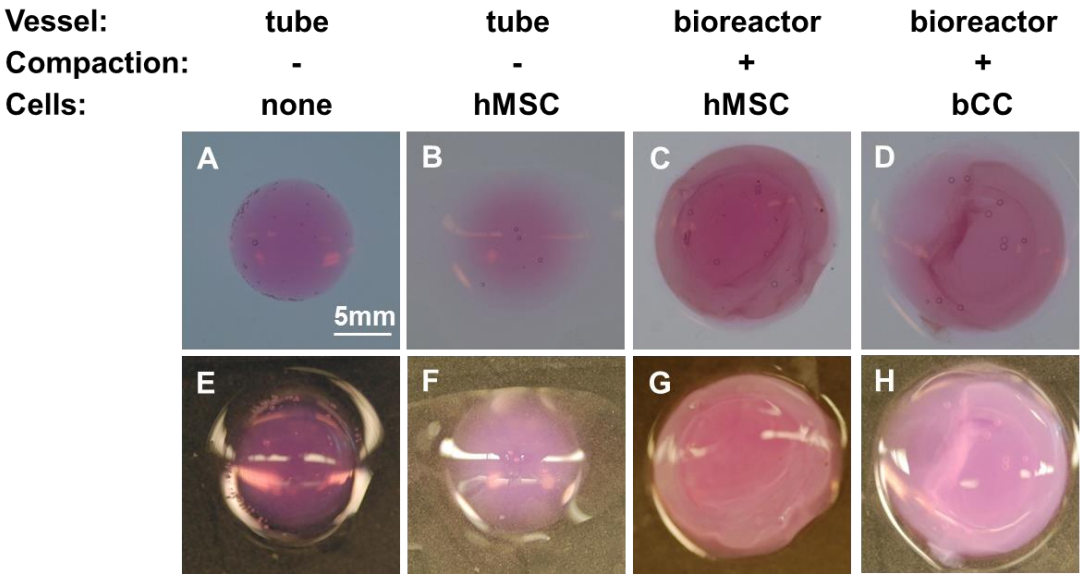

Figure 3.6. Collagen constructs of permeation compaction. Collagen gels were formed with **(A,E)** no cells and no compaction, **(B,F)** hMSC and no compaction, **(C,G)** hMSC and permeation compaction, and **(D,H)** bCC and permeation compaction. **(A-D)** Light background for opacity. **(E-H)** Solid background.

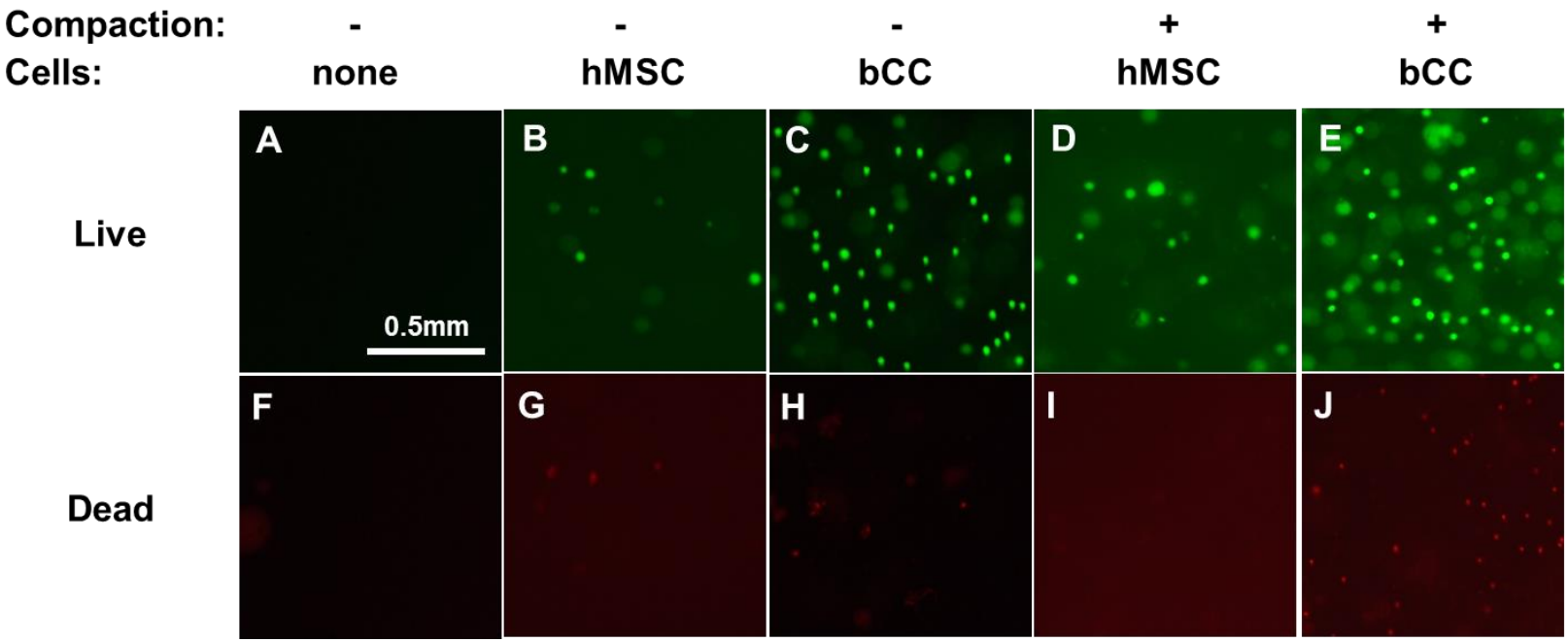

Figure 3.7. Effects of permeation compaction on cell viability. **(A-E)** Green fluorescence indicating live cells. **(F-J)** Red fluorescence indicating the nuclei of dead cells. **(A,F)** No cell was seeded. Collagen gels were seeded with **(B,G)** hMSCs and **(C,H)** bCCs but were not compacted Collagen gels were seeded with **(D,I)** hMSCs and **(E,J)** bCCs but were compacted

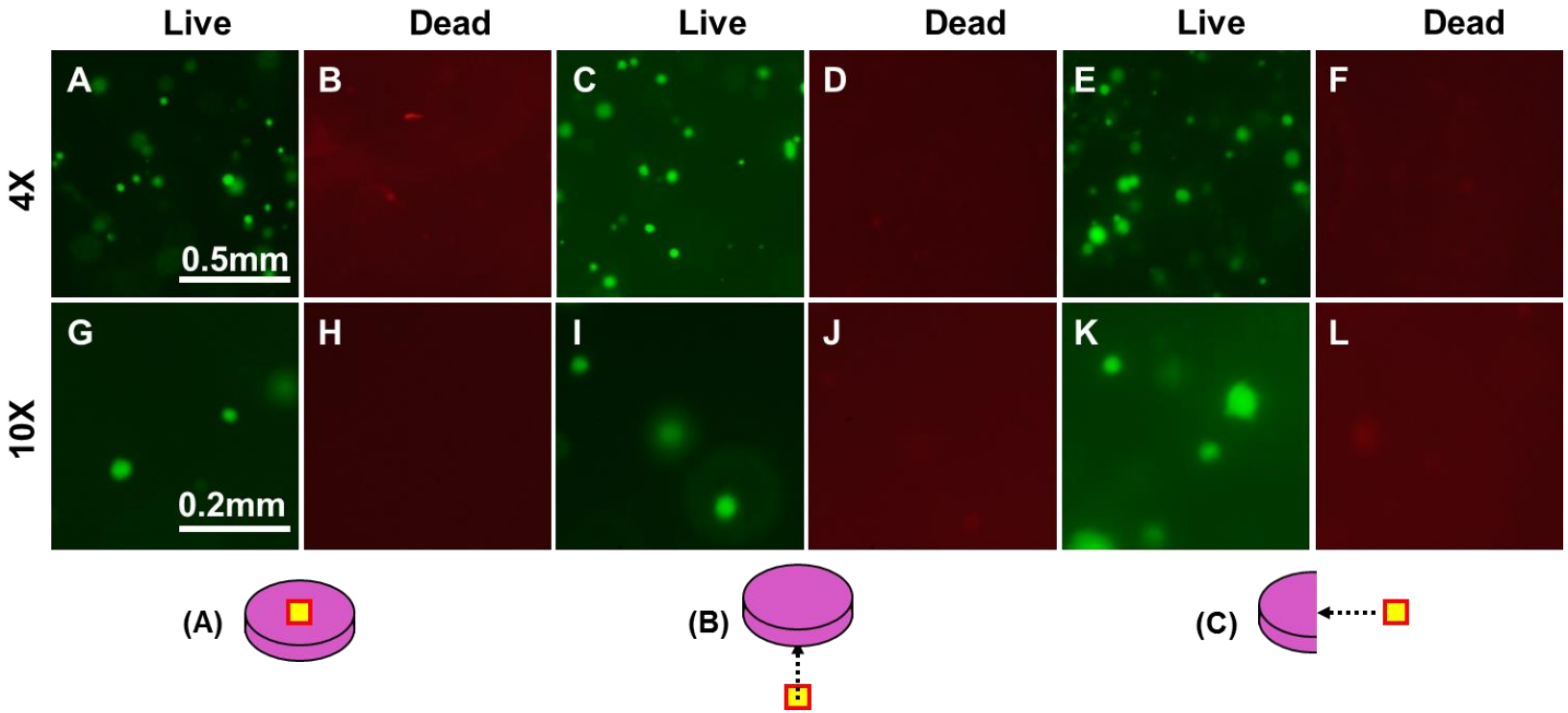

Figure 3.8. Effects of permeation compaction (hMSC). Live/dead images were taken at **(A, B, G, H)** top, **(C,D,I,J)** bottom, and **(E,F,K,L)** cross section of the construct.

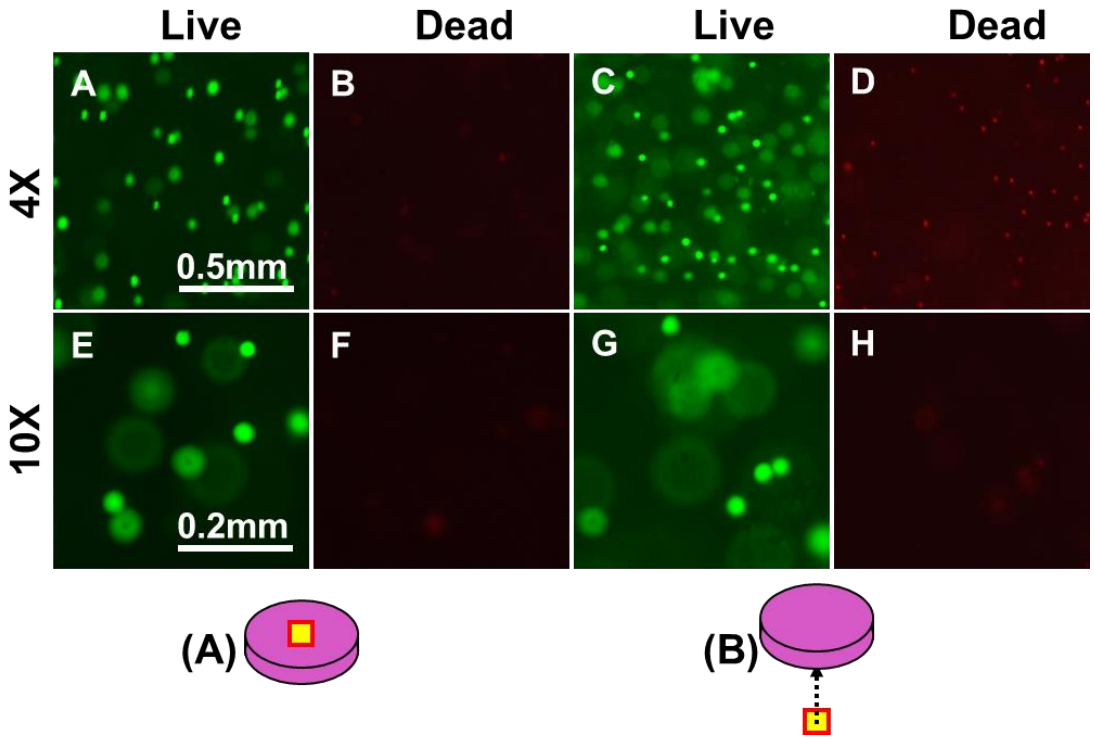

Figure 3.9.Effects of permeation compaction (bCC). Live/dead images were taken at **(A,B,E,F)** top and **(C,D,G,H)** bottom of the construct.

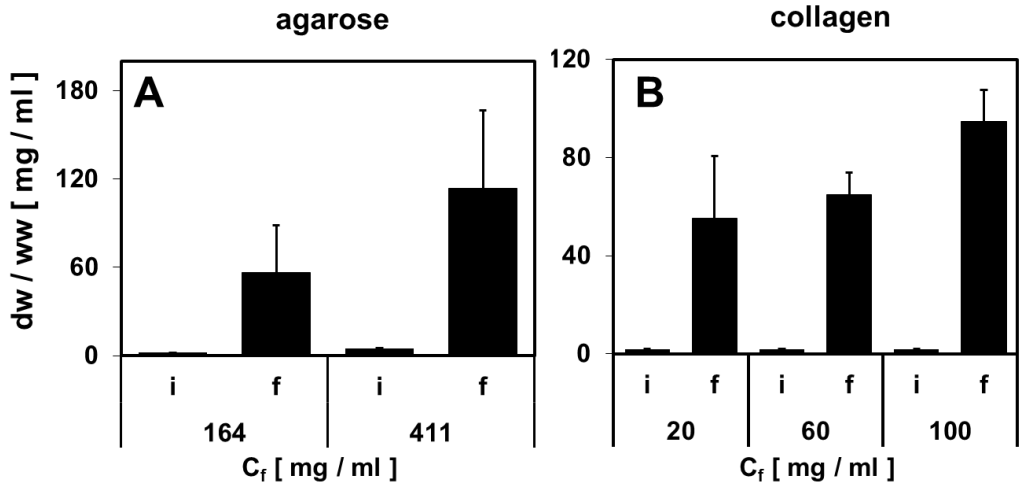

Figure 3.10. Comparison (direct compaction) of dw / ww before and after compaction. The error bars represent sd. i: initial concentration before compaction. f: final concentration after compaction

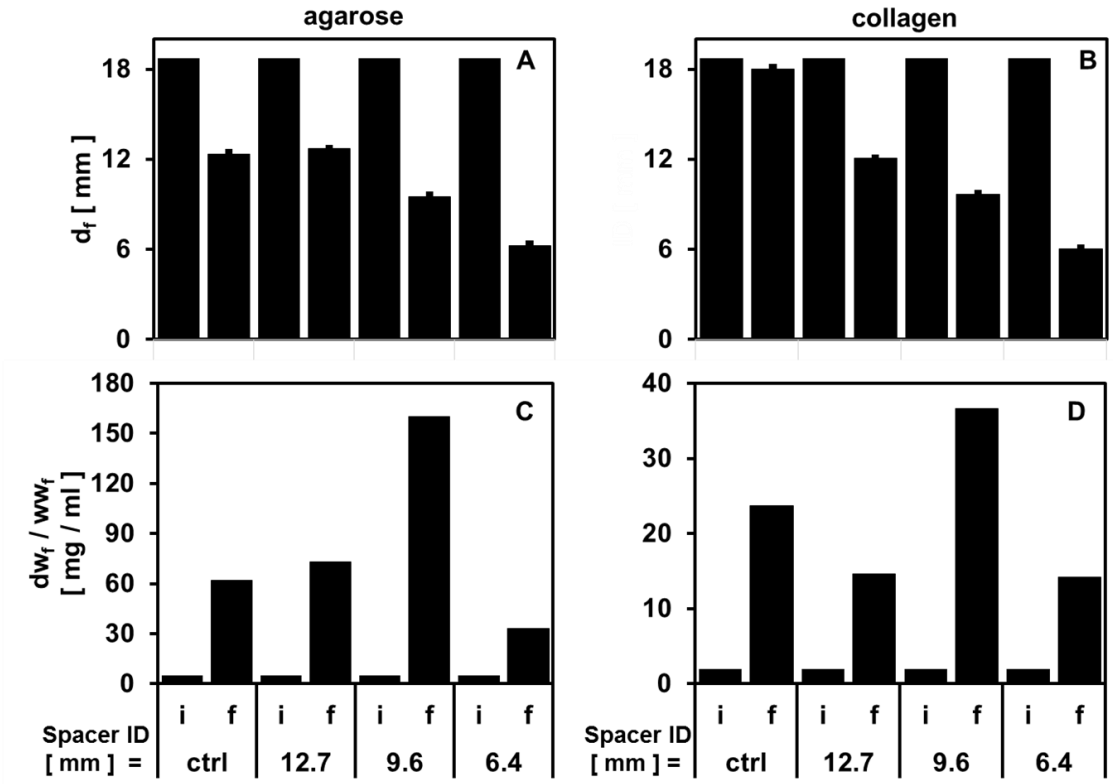

Figure 3.11. Effects of spacer on structure and composition. i: initial/before compaction, f: final/after compaction, ctrl: control. The final diameter, d_f, and dry to wet weight ratio, dw_f / ww_f, of **(A,C)** agarose and **(B,D)** collagen constructs were measured before compaction, i, and after compaction, f.

B. Tables

Table 3.1. Physical properties for direct compacted agarose disks. Definitions of parameters: H_{A0}: confined compression modulus, k_p: permeability constant, e: strain. Data was presented as mean±sd, n=3.

Exp / Group		**I / 01**	**I / 02**
C_i , $C_{f,target}$ [mg / ml]		2 , 164	5 , 411
m_i [mg]		25	63
h_i [mm]		46	46
After compaction	**h_f [mm]**	1.34±0.98	2.10±0.89
	ww_f [mg]	191±104	430±245
After swelling	**h_f [mm]**	1.40±1.08	2.47±0.82
	ww_f [mg]	236±131	522±280
Final	**dw_f [mg]**	9.1±3.8	40.3±11.5
	dw_f / ww_f [%]	5.6±3.2	11.4±5.3
Confined compression testing	**H_{A0} [kPa]**	24±19	87±108
	k_{p0} @e=0 [10^{-15} m^2 / (Pa·s)]	4,830±8180	89±94
	k_p@e=0.2 [10^{-15} m^2 / (Pa·s)]	351±562	1.8±1.7
	k_p @e=0.4 [10^{-15} m^2 / (Pa·s)]	27.5±35.2	8.9±10.0

Table 3.2. Physical properties for direct compacted collagen disks.*II/01 samples were untestable due to their soft and fragile characteristics. Definitions of parameters: H_{A0}: confined compression modulus, k_p: permeability constant, e: strain, max load: maximum recorded load, peak stress: maximum stress prior to failure, elongation at failure: elongation at maximum load, failure strain: (elongation at failure-tare displacement)/gauge length, stiffness at failure strain: peak stress/failure strain. Data was presented as mean±sd, n=3.

Exp / Group		**II / 01***	**II / 02**	**II / 03**
C_i , C_f [mg / ml]		2, 20	2, 60	2, 100
m_i [mg]		3.1	9.1	15.2
h_i [mm]		5.53	16.6	27.7
After compaction	**h_f [mm]**	0.13±0.04	0.64±0.19	0.73±0.25
	ww_f [mg]	90.1±3.9	173±22.3	193±10.3
After swelling	**h_f [mm]**	0.10±0.17	0.61±0.16	0.86±0.28
	ww_f [mg]	67.4±44.1	183±19.5	266±24.8
Final	**dw_f [mg]**	5.0±2.3	11.2±2.0	18.2±1.6
	dw_f / ww_f [%]	5.5±2.5	6.5±0.9	9.5±1.3
Confined compression testing	**H_{A0} [kPa]**	-	0.42±0.11	0.85±0.63
	k_{p0}@e=0 [10^{-15} m^2 / (Pa·s)]	-	1720±1800	2880±270
	k_p@e=0.2 [10^{-15} m^2 / (Pa·s)]	-	410±450	1000±10
	kp@e=0.4 [10^{-15} m^2 / (Pa·s)]	-	340±340	340±40
Tensile testing	**Max load [mN]**	-	49.5±1.3	114.0±21.9
	Peak stress[MPa]	-	0.08±0.06	0.10±0.01
	Elongation at failure [mm]	-	2.1±0.8	3.6±1.4
	Failure strain	-	0.44±0.18	0.84±0.42
	Stiffness at failure strain [MPa]	-	0.26±0.32	0.13±0.06

Table 3.3. Effects of direct compaction on cell viability. C_i: initial concentration of collagen. C_f: final/target concentration of collagen.

Exp	Group	C_i [mg / ml]	C_f [mg / ml]	Cell type	Viability [%]
III	**01**	2	2	-	N/A
	02	2	2	bCC	99.0
	03	2	2	hMSC	95.0
	04	2	20	bCC	0
	05	2	20	hMSC	7.3

Table 3.4. Numerical results and analysis on structure and composition of constructs with spacers. ID: inner diameter. C_i: initial concentration. C_f: final concentration. ww: wet weight. dw: dry weight.

Exp / Group	IV / 02	IV / 03	IV / 04	IV / 05	V / 02	V / 03	V / 04	V / 05
Material	**agarose**				**collagen**			
Spacer h [mm]	1.50	3.18			1.50	3.18		
Spacer ID [mm]	12.7	12.7	9.6	6.4	12.7	12.7	9.6	6.4
C_i [mg / ml]	5	5	5	5	2	2	2	2
m_i [mg]	63	63	63	63	3.1	3.1	3.1	3.1
$C_{f,target}$ [mg / ml]	417	156	272	625	20	7.5	13.2	29.7
$C_{f,target}$ / C_i	83	31	54	125	10.0	3.8	6.6	14.9
h_i [mm]	46.2	46.2	46.2	46.2	5.53	5.53	5.53	5.53
h_f [mm]	2.34±0.16	3.61±0.10	3.55±0.16	2.53±0.16	0.19±0.04	1.01±0.19	1.27±0.10	1.06±0.20
d_f [mm]	12.3±0.1	12.7±0.2	9.5±0.1	6.3±0.2	18.0±0.2	12.1±0.6	9.6±0.2	6.0±0.3
V_f [mm^3]	278	457	252	78.9	48.3	116	91.9	30.0
ww_f [mg]	439	522	345	98.2	160	103	57.3	56.2
dw_f [mg]	27.2	38.0	55.2	3.2	3.8	1.5	2.1	0.8
dw_f / ww_f [%]	6.2	7.3	16	3.3	2.4	1.5	3.7	1.4
h_i / h_f	19.7	12.8	13.0	18.3	29.1	5.48	4.35	5.22
dw_f / m_i	0.43	0.60	0.88	0.05	1.23	0.48	0.68	0.26
(dw_f / V_f) / C_i	20	17	44	8.1	39	6.5	11	13

Table 3.5. Cell viability result (permeation compaction). C_i: initial concentration of collagen. C_f: final/target concentration of collagen.

Exp	Group	C_i [mg / ml]	C_f [mg / ml]	Cell type	dw / ww [mg / ml]	Viability [%]
V	**01**	2	2	-	-	N/A
	02	2	2	hMSC	-	80
	03	2	2	bCC	-	90
	04	2	40	hMSC	86	71
	05	2	40	bCC	28	62

Table 3.6. Compaction studies in comparison. This table summarizes the variables in other studies compared with this study.

Study	Independent Var.				Dependent Var.	
	Method	**Shape**	**Pore size [µm]**	**Material**	**C_f [mg / ml]**	**Cell**
Brown et al	unconfined compression	rectangular	50	col type I	n/d	n/d
Han et al	confined compression	circular	2	agarose col type II	25	viable
Blum et al		rectangular, circular	50	collagen oligomer	3.5-24.5	viable
Sungil	confined compression	circular	0.2	agarose col type I	60 – 120 20 – 100	not viable
	permeation	circular		col type I	40	viable

DISCUSSION

This thesis paper examined the ability of a bioreactor to achieve compaction of hydrogels by direct compaction with a constant pressure (180 kPa) or permeation compaction with an applied constant fluid flow (43 µl/min). The shape of final constructs was circular disc with different opacity and affected by the presence of spacers. Both compactions resulted in increase in dw/ww ratio although the target concentration and complete retention of materials were not achieved. The mechanical properties including compressive modulus and hydraulic permeability were varied with target construct and material. The effects of direct and permeation compaction on cell viability were markedly different; high cell viability was only observed in constructs compacted via permeation.

These studies provide various engineering tools that can be useful in making cartilaginous constructs. The successful use of commercial telocollagen type I in the bioreactor is advantageous for its simplicity and cost-effectiveness. A novel permeation method in addition to direct compaction is easily adopted for various experimental designs. With 0.2 µm pore size filter, many fibrous hydrogels whose diameter is smaller can be tested as well. Although concentrations and dimensions of constructs may be controlled with spacer, more studies are needed to improve the accuracy of controllable measures.

The pressure gradients associated with direct and permeation compaction can be compared. Static load of 180 kPa was practically set for

steady and complete direct compaction. The pressure gradient through the collagen scaffold due to fluid flow can be found using Darcy's law [36]

$$\upsilon = \frac{\kappa \Delta P}{\mu L} \quad (1)$$

where ν is the fluid velocity, κ is the hydraulic permeability, μ is the viscosity, P is the pressure, and L is the thickness of a slab. Also, κ for 3D arrays of fibers can be found by the equation derived by Jackson and James [35]

$$\frac{\kappa}{a^2} = -\frac{3}{20\phi}(\ln \phi + 0.931) \quad (2)$$

where a is the fiber radius and ϕ is the volume fraction of fibers. Using the reported values of a (0.17 μm) and, assuming that rho = 1.025 g / cm^3 and C_{col} = 2 – 40 mg/ml, the calculated ϕ ranges from -3.0*10^{-13} to -1.4*10^{-11} for collagen in hydrogel [36, 68] and the viscosity is that of water (0.001 N s / m^2), the calculated ΔP, based on equation 1 and 2, ranges from -200 to -5 Pa. As a result, permeation compaction creates negative pressure across the scaffold. Thus, the pressure gradient across the sample with permeation compaction (5-200 Pa), is much less than that with direct compaction (180 kPa).

Reported typical values of H_A and k_p for AC are in the range of 0.5 – 0.9 MPa and 1x10^{-16} – 1x10^{-15} m^2/(Pa·s), respectively [7]. The H_A and k_p of compacted constructs show the potential for obtaining biomechanical properties similar to natural articular cartilage. However, the tensile modulus was not close to the reported value (5 – 25 MPa) [6]. Discrepancy may be due to the absence

of PG in scaffold since the tensile modulus of ECM to collagen to PG ratio is strongly correlated [1].

Permeation compaction creates a compacted collagen construct with viable cells with possibility to enhance biomimetic properties of the dense scaffold. Density difference within the construct (Figure 3.7 (C)) is caused by uneven outflow on the FLS during the compaction as the dense region for VI/04 and VI/05 appeared at the center where the 12.7mm diameter filter was. This suggests that the outflow of fluid occurred unevenly over the entire construct. If so, control of outflow can be achieved by the filter and the creation of a density gradient within the construct that can induce cell migration may be achieved [22]. The morphology of cells determined from calcein AM staining of cell cytoplasm showed that all the cells were circular, suggesting that cell adhesion onto the collagen fibrils did not fully take place [37]. Closer image of hMSC (Figure 3.9 (K)) indicates spreading of cells to the collagen fibers, as change in cell morphology in flattened spindle or discoid shapes [22] can be observed within a day of culture in high dense collagen construct [12].

During the compaction, the media is filtered through three networks: First, 40 µm pore size mesh, second, 0.2 µm pore size membrane, and lastly, 2 µm frit. These filter sizes act as semi-permeable membrane that entraps the constituents of construct, resulting in irreversible compaction. However, during agarose compaction, those fibers smaller than the pore sizes of filters can escape the confined chamber as leakage of agarose through top chamber was

observed. Inconsistency in structure and composition of constructs as well as irreversibility of compaction also suggests that the random entanglements of fibers seem to play a role. Moreover, fiber-fiber interaction can cause coulombic friction, affecting the rheological behavior and irreversibility [64].

Cell viability was assessed on the compacted constructs with bCC and hMSC. The fluorescence dyes, calcein acetoxymethyl (calcein AM) and ethidium homodimer-1, stain cell cytoplasm in live cells and DNA in dead cells while they excite and emit at 494/517 and 528/617 nm (excitation/emission), seen as green and red color under fluorescence microscope, respectively. Since calcein AM and ethidium homodimer-1 stain cell cytoplasm and DNA in nucleus, respectively, the results of the assay for proper staining can be verified approximately by comparing the size of the diameter of cells (10-30μm) and nucleus (3-10μm). No or low viability after the direct compaction may be due to the insufficient protective materials such as PG and/or ECM for cells from shear flow since apoptosis or necrotic cell death can be induced by shear flow of 1 Pa and 2 Pa for single cell [69]. In addition, cells may be particularly sensitive to dehydration and hypo-osmotic damage in the low mass of the collagen sheet [14]. This indicates that less pressure and shear flow when compacting to create a cellularized construct may minimize the cell death after compaction.

CONCLUSION

Direct compaction in the bioreactor can produce structurally rigid and compacted collagen constructs with various densities. The biomechanical properties of the constructs were as similar as a natural tissue to a certain degree but they must be further improved and investigated for cell encapsulation. The study with designed spacers for uniaxial loading showed potential that such molding technique could be applied for a compacted construct, either agarose or collagen. Permeation compaction in the bioreactor resulted in successful fabrication of a high density collagen construct from commercial acid-soluble telocollagen and cellularized with various types of cells including hMSCs and bCCs, both of which serve as potential sources for therapeutic cell populations, without significant decreases in cell viability [30]. Use of the bioreactor designed by the senior design team 2014-2015 in the CTE lab allows the production of dense collagen tissues via compaction method, either with piston (direct) or pump (permeation). Permeation compaction method not only produces a compacted collagen scaffold, but also increases cell viability of the construct necessary for successful engineered cartilage tissues. These properties are advantageous for creating a biomimetic tissue graft. In future, the effects of collagen density as well as ECM formation and secretion by seeded cells on the biomechanical properties of a compacted collagen construct should be studied. In addition, the comparison of biomechanical properties of constructs via direct and permeation compaction

may be helpful to figure out the underlying mechanism of compaction at molecular level. Understanding cellular activities in 3D dense scaffold, whether agarose or collagen, should be achieved as well.

REFERENCES

1. Akizuki S, Mow VC, Müller F, Pita JC, Howell DS, Manicourt DH: Tensile properties of human knee joint cartilage: I. Influence of ionic conditions, weight bearing, and fibrillation on the tensile modulus. *Journal of Orthopaedic Research* 4:379-92, 1986.

2. Alford JW, Cole BJ: Cartilage restoration, part 1: basic science, historical perspective, patient evaluation, and treatment options. *Am J Sports Med* 33:295-306, 2005.

3. Alini M, Li W, Markovic P, Aebi M, Spiro RC, Roughley PJ: The Potential and Limitations of a Cell-Seeded Collagen/Hyaluronan Scaffold to Engineer an Intervertebral Disc-Like Matrix. *Spine* 28, 2003.

4. Armstrong CG, Mow VC: Variations in the intrinsic mechanical properties of human articular cartilage with age, degeneration, and water content. *J Bone Joint Surg Am* 64:88-94, 1982.

5. Aroen A, Loken S, Heir S, Alvik E, Ekeland A, Granlund OG, Engebretsen L: Articular cartilage lesions in 993 consecutive knee arthroscopies. *Am J Sports Med* 32:211-5, 2004.

6. Athanasiou KA, Darling EM, Hu JC: Articular Cartilage Tissue Engineering. *Synthesis Lectures on Tissue Engineering* 1:1-182, 2009.

7. Athanasiou KA, Rosenwasser MP, Buckwalter JA, Malinin TI, Mow VC: Interspecies comparisons of in situ intrinsic mechanical properties of distal femoral cartilage. *J Orthop Res* 9:330-40, 1991.

8. Awad HA, Wickham MQ, Leddy HA, Gimble JM, Guilak F: Chondrogenic differentiation of adipose-derived adult stem cells in agarose, alginate, and gelatin scaffolds. *Biomaterials* 25:3211-22, 2004.

9. Bentley G, Biant LC, Vijayan S, Macmull S, Skinner JA, Carrington RW: Minimum ten-year results of a prospective randomised study of autologous chondrocyte implantation versus mosaicplasty for symptomatic articular cartilage lesions of the knee. *J Bone Joint Surg Br* 94:504-9, 2012.

10. Benya PD, Shaffer JD: Dedifferentiated chondrocytes reexpress the differentiated collagen phenotype when cultured in agarose gels. *Cell* 30:215-24, 1982.

11. Bhosale AM, Richardson JB: Articular cartilage: structure, injuries and review of management. *Br Med Bull* 87:77-95, 2008.

12. Blum KM, Novak T, Watkins L, Neu CP, Wallace JM, Bart ZR, Voytik-Harbin SL: Acellular and cellular high-density, collagen-fibril constructs with suprafibrillar organization. *Biomater Sci* 4:711-23, 2016.

13. Brittberg M, Lindahl A, Nilsson A, Ohlsson C, Isaksson O, Peterson L: Treatment of deep cartilage defects in the knee with autologous chondrocyte transplantation. *N Engl J Med* 331:889-95, 1994.

14. Brown RA, Wiseman M, Chuo CB, Cheema U, Nazhat SN: Ultrarapid Engineering of Biomimetic Materials and Tissues: Fabrication of Nano and Microstructures by Plastic Compression. *Advanced Functional Materials* 15:1762-70, 2005.

15. BUCKWALTER JA, MANKIN HJ: Instructional Course Lectures, The American Academy of Orthopaedic Surgeons - Articular Cartilage. Part I: Tissue Design and Chondrocyte-Matrix Interactions*†. *The Journal of Bone & Joint Surgery* 79:600-11, 1997.

16. Buckwalter JA, Mow VC, Ratcliffe A: Restoration of Injured or Degenerated Articular Cartilage. *J Am Acad Orthop Surg* 2:192-201, 1994.

17. Buschmann MD, Gluzband YA, Grodzinsky AJ, Kimura JH, Hunziker EB: Chondrocytes in agarose culture synthesize a mechanically functional extracellular matrix. *Journal of Orthopaedic Research* 10:745-58, 1992.

18. Buschmann MD, Gluzband YA, Grodzinsky AJ, Kimura JH, Hunziker EB: Chondrocytes in agarose culture synthesize a mechanically functional extracellular matrix. *J Orthop Res* 10:745-58, 1992.

19. Caplan AI: Adult mesenchymal stem cells for tissue engineering versus regenerative medicine. *J Cell Physiol* 213:341-7, 2007.

20. Chaipinyo K, Oakes BW, Van Damme MP: The use of debrided human articular cartilage for autologous chondrocyte implantation: maintenance of chondrocyte differentiation and proliferation in type I collagen gels. *J Orthop Res* 22:446-55, 2004.

21. Chang SC, Rowley JA, Tobias G, Genes NG, Roy AK, Mooney DJ, Vacanti CA, Bonassar LJ: Injection molding of chondrocyte/alginate constructs in the shape of facial implants. *J Biomed Mater Res* 55:503-11, 2001.

22. Cheema U, Brown RA: Rapid Fabrication of Living Tissue Models by Collagen Plastic Compression: Understanding Three-Dimensional Cell Matrix Repair In Vitro. *Adv Wound Care (New Rochelle)* 2:176-84, 2013.

23. Chiang H, Jiang CC: Repair of articular cartilage defects: review and perspectives. *J Formos Med Assoc* 108:87-101, 2009.

24. Desjardins MR, Hurtig MB: Cartilage healing: A review with emphasis on the equine model. *Can Vet J* 31:565-72, 1990.

25. Eyre D: Collagen of articular cartilage. *Arthritis Res* 4:30-5, 2002.

26. Eyre DR WJ. Type XI or 1α2α3α collagen. In Structure and Function of Collagen Types. In: BR Mayne R, ed.: New York: Academic Press; 1987:261-81.

27. Feng Z, Yamato M, Akutsu T, Nakamura T, Okano T, Umezu M: Investigation on the mechanical properties of contracted collagen gels as a scaffold for tissue engineering. *Artif Organs* 27:84-91, 2003.

28. Guilak F, Ratcliffe A, Lane N, Rosenwasser MP, Mow VC: Mechanical and biochemical changes in the superficial zone of articular cartilage in canine experimental osteoarthritis. *J Orthop Res* 12:474-84, 1994.

29. Han E, Wilensky LM, Schumacher BL, Chen AC, Masuda K, Sah RL: Tissue engineering by molecular disassembly and reassembly: biomimetic retention of mechanically functional aggrecan in hydrogel. *Tissue Engineering Part C: Methods* 16:1471-9, 2010.

30. Han EH, Ge C, Chen AC, Schumacher BL, Sah RL: Compaction enhances extracellular matrix content and mechanical properties of tissue-engineered cartilaginous constructs. *Tissue Eng Part A* 18:1151-60, 2012.

31. Heir S, Nerhus TK, Rotterud JH, Loken S, Ekeland A, Engebretsen L, Aroen A: Focal cartilage defects in the knee impair quality of life as much as severe osteoarthritis: a comparison of knee injury and osteoarthritis outcome score in 4 patient categories scheduled for knee surgery. *Am J Sports Med* 38:231-7, 2010.

32. Hjelle K, Solheim E, Strand T, Muri R, Brittberg M: Articular cartilage defects in 1,000 knee arthroscopies. *Arthroscopy* 18:730-4, 2002.

33. Hollister SJ: Porous scaffold design for tissue engineering. *Nat Mater* 4:518-24, 2005.

34. Huang D, Chang TR, Aggarwal A, Lee RC, Ehrlich HP: Mechanisms and dynamics of mechanical strengthening in ligament-equivalent fibroblast-populated collagen matrices. *Ann Biomed Eng* 21:289-305, 1993.

35. Jackson GW, James DF: The permeability of fibrous porous media. *The Canadian Journal of Chemical Engineering* 64:364-74, 1986.

36. Johnson EM, Deen WM: Hydraulic permeability of agarose gels. *AIChE Journal* 42:1220-4, 1996.

37. Jokinen J, Dadu E, Nykvist P, Kapyla J, White DJ, Ivaska J, Vehvilainen P, Reunanen H, Larjava H, Hakkinen L, Heino J: Integrin-mediated cell adhesion to type I collagen fibrils. *J Biol Chem* 279:31956-63, 2004.

38. Kadiyala S, Jaiswal N, Bruder SP: Culture-expanded, bone marrow-derived mesenchymal stem cells can regenerate a critical-sized segmental bone defect. *Tissue engineering* 3:173-85, 1997.

39. Klein T, Sah R: Modulation of depth-dependent properties in tissue-engineered cartilage with a semi-permeable membrane and perfusion: a continuum model of matrix metabolism and transport. *Biomechanics and modeling in mechanobiology* 6:21-32, 2007.

40. Knutsen G, Engebretsen L, Ludvigsen TC, Drogset JO, Grontvedt T, Solheim E, Strand T, Roberts S, Isaksen V, Johansen O: Autologous chondrocyte implantation compared with microfracture in the knee. A randomized trial. *J Bone Joint Surg Am* 86-a:455-64, 2004.

41. Krishnan L, Weiss JA, Wessman MD, Hoying JB: Design and application of a test system for viscoelastic characterization of collagen gels. *Tissue Eng* 10:241-52, 2004.

42. Lahiji A, Sohrabi A, Hungerford DS, Frondoza CG: Chitosan supports the expression of extracellular matrix proteins in human osteoblasts and chondrocytes. *Journal of biomedical materials research* 51:586-95, 2000.

43. Lai W, Mow VC, Roth V: Effects of nonlinear strain-dependent permeability and rate of compression on the stress behavior of articular cartilage. *Journal of biomechanical engineering* 103:61-6, 1981.

44. Lefebvre V, Peeters-Joris C, Vaes G: Production of collagens, collagenase and collagenase inhibitor during the dedifferentiation of articular chondrocytes by serial subcultures. *Biochim Biophys Acta* 1051:266-75, 1990.

45. Ma PX, Langer R: Morphology and mechanical function of long-term in vitro engineered cartilage. *Journal of biomedical materials research* 44:217-21, 1999.

46. Mankin HJ: The reaction of articular cartilage to injury and osteoarthritis (first of two parts). *N Engl J Med* 291:1285-92, 1974.

47. Mankin HJ, Thrasher AZ: Water content and binding in normal and osteoarthritic human cartilage. *J Bone Joint Surg Am* 57:76-80, 1975.

48. Maroudas A, Bullough P, Swanson S, Freeman M: The permeability of articular cartilage. *Bone & Joint Journal* 50:166-77, 1968.

49. Mauck RL, Seyhan SL, Ateshian GA, Hung CT: Influence of seeding density and dynamic deformational loading on the developing structure/function relationships of chondrocyte-seeded agarose hydrogels. *Ann Biomed Eng* 30:1046-56, 2002.

50. Mauck RL, Wang CC, Oswald ES, Ateshian GA, Hung CT: The role of cell seeding density and nutrient supply for articular cartilage tissue engineering with deformational loading. *Osteoarthritis Cartilage* 11:879-90, 2003.

51. Mow VC, Holmes MH, Michael Lai W: Fluid transport and mechanical properties of articular cartilage: A review. *Journal of Biomechanics* 17:377-94, 1984.

52. Mow VC, Kuei S, Lai WM, Armstrong CG: Biphasic creep and stress relaxation of articular cartilage in compression: theory and experiments. *Journal of biomechanical engineering* 102:73-84, 1980.

53. Muir H: The chondrocyte, architect of cartilage. Biomechanics, structure, function and molecular biology of cartilage matrix macromolecules. *Bioessays* 17:1039-48, 1995.

54. Nehrer S, Breinan HA, Ramappa A, Hsu HP, Minas T, Shortkroff S, Sledge CB, Yannas IV, Spector M: Chondrocyte-seeded collagen matrices implanted in a chondral defect in a canine model. *Biomaterials* 19:2313-28, 1998.

55. O'Brien FJ, Harley B, Yannas IV, Gibson LJ: The effect of pore size on cell adhesion in collagen-GAG scaffolds. *Biomaterials* 26:433-41, 2005.

56. Peterson L, Minas T, Brittberg M, Lindahl A: Treatment of osteochondritis dissecans of the knee with autologous chondrocyte transplantation: results at two to ten years. *J Bone Joint Surg Am* 85-A Suppl 2:17-24, 2003.

57. Pittenger MF, Mackay AM, Beck SC, Jaiswal RK, Douglas R, Mosca JD, Moorman MA, Simonetti DW, Craig S, Marshak DR: Multilineage potential of adult human mesenchymal stem cells. *Science* 284:143-7, 1999.

58. Radice M, Brun P, Cortivo R, Scapinelli R, Battaliard C, Abatangelo G: Hyaluronan-based biopolymers as delivery vehicles for bone-marrow-derived mesenchymal progenitors. *Journal of biomedical materials research* 50:101-9, 2000.

59. Revell CM, Athanasiou KA: Success Rates and Immunologic Responses of Autogenic, Allogenic, and Xenogenic Treatments to Repair Articular Cartilage Defects. *Tissue Eng Part B Rev* 15:1-15, 2009.

60. Richter DL, Schenck RC, Jr., Wascher DC, Treme G: Knee Articular Cartilage Repair and Restoration Techniques: A Review of the Literature. *Sports Health* 8:153-60, 2016.

61. Ringe J, Burmester GR, Sittinger M: Regenerative medicine in rheumatic disease[mdash]progress in tissue engineering. *Nat Rev Rheumatol* 8:493-8, 2012.

62. Rowley JA, Madlambayan G, Mooney DJ: Alginate hydrogels as synthetic extracellular matrix materials. *Biomaterials* 20:45-53, 1999.

63. Sechriest VF, Miao YJ, Niyibizi C, Westerhausen-Larson A, Matthew HW, Evans CH, Fu FH, Suh J-K: GAG-augmented polysaccharide hydrogel: a novel biocompatible and biodegradable material to support chondrogenesis. *Journal of biomedical materials research* 49:534-41, 2000.

64. Servais C, Månson J-AE, Toll S: Fiber–fiber interaction in concentrated suspensions: Disperse fibers. *Journal of Rheology* 43:991-1004, 1999.

65. Sgaglione NA, Miniaci A, Gillogly SD, Carter TR: Update on advanced surgical techniques in the treatment of traumatic focal articular cartilage lesions in the knee. *Arthroscopy* 18:9-32.

66. Sittinger M, Reitzel D, Dauner M, Hierlemann H, Hammer C, Kastenbauer E, Planck H, Burmester G, Bujia J: Resorbable polyesters in cartilage engineering: affinity and biocompatibility of polymer fiber structures to chondrocytes. *Journal of biomedical materials research* 33:57-63, 1996.

67. Sophia Fox AJ, Bedi A, Rodeo SA: The Basic Science of Articular Cartilage: Structure, Composition, and Function. *Sports Health* 1:461-8, 2009.

68. Stylianopoulos T, Diop-Frimpong B, Munn LL, Jain RK: Diffusion anisotropy in collagen gels and tumors: the effect of fiber network orientation. *Biophysical journal* 99:3119-28, 2010.

69. Tanzeglock T, Soos M, Stephanopoulos G, Morbidelli M: Induction of mammalian cell death by simple shear and extensional flows. *Biotechnol Bioeng* 104:360-70, 2009.

70. Temenoff JS, Mikos AG: Review: tissue engineering for regeneration of articular cartilage. *Biomaterials* 21:431-40, 2000.

71. Vunjak-Novakovic G, Martin I, Obradovic B, Treppo S, Grodzinsky AJ, Langer R, Freed LE: Bioreactor cultivation conditions modulate the composition and mechanical properties of tissue-engineered cartilage. *J Orthop Res* 17:130-8, 1999.

72. Wei X, Yang X, Han Z-p, Qu F-f, Shao L, Shi Y-f: Mesenchymal stem cells: a new trend for cell therapy. *Acta Pharmacol Sin* 34:747-54, 2013.

73. Widuchowski W, Widuchowski J, Trzaska T: Articular cartilage defects: study of 25,124 knee arthroscopies. *Knee* 14:177-82, 2007.

74. Williamson AK, Chen AC, Masuda K, Thonar EJ, Sah RL: Tensile mechanical properties of bovine articular cartilage: variations with growth and relationships to collagen network components. *J Orthop Res* 21:872-80, 2003.

75. Williamson AK, Chen AC, Sah RL: Compressive properties and function-composition relationships of developing bovine articular cartilage. *J Orthop Res* 19:1113-21, 2001.